

The [OIII] Emission-line Nebula of the $z = 3.594$ Radio Galaxy 4C +19.71*

L. Armus¹, B.T. Soifer, T.W. Murphy Jr., G. Neugebauer, A.S. Evans & K. Matthews

Palomar Observatory, Caltech, Pasadena, CA 91125

¹ Current Address, Infrared Processing and Analysis Center, Caltech 100-22, Pasadena, CA 91125

* Based on observations at the W.M. Keck Observatory, which is operated by the California
Institute of Technology and the University of California

Received _____; accepted _____

ABSTRACT

We have imaged the $z = 3.594$ radio galaxy 4C +19.71 in the light of the redshifted [OIII] 5007Å emission line, using a narrow-band filter centered at $2.3\mu\text{m}$ with the Near Infrared Camera on the Keck Telescope. The [OIII] nebula of 4C +19.71 has a size of 74×9 kpc, and a luminosity of $L_{5007} \sim 3 \times 10^{37}$ W. The rest frame equivalent width of the 5007Å line, averaged over the entire nebula, is 560Å. The length of the major axis of the [OIII] emission is nearly identical to the separation of the radio lobes seen at 1465 MHz (Rottgering, et al. 1994), and the position angle of the nebula is the same as that of the two radio lobes. In addition, 4C +19.71 follows the optical emission line vs. radio power correlation seen in other powerful radio galaxies. The [OIII] and Ly α emission-line luminosities suggest that the ionized gas mass lies in the range of $2 \times 10^8 - 10^9 M_{\odot}$. The O/H ratio in the nebula is at least a few tenths solar, and may be as high as a factor of three above solar, indicating a previous phase of star formation in 4C +19.71. Thirty five percent of the total K-band flux is contributed by the 5007Å emission line, and the continuum of 4C +19.71 has a $K \sim 19.6$ mag. This places 4C +19.71 along the K-z relation found for other radio galaxies and radio loud quasars. If the continuum is dominated by starlight, the host galaxy has a rest frame visual luminosity of about $40L^*$. There are no candidate emission-line objects at the redshift of 4C +19.71 having [OIII] rest frame equivalent widths of more than about 2% that of the radio galaxy itself within a volume of 212 Mpc^3 .

Subject headings: Galaxies: General, Galaxies: Individual - 4C19.71, Galaxies: photometry - infrared

1. Introduction

A ubiquitous feature in the spectra of powerful radio galaxies is the presence of bright ultraviolet and optical emission lines. These lines can be quite strong, with rest frame equivalent widths of several hundred angstroms. The strength of the emission lines, coupled with the large sky coverage of radio surveys, has facilitated the discovery of radio galaxies over a large range in redshift. As a result, powerful radio galaxies are among the most extensively studied stellar systems at moderate and high redshifts.

By observing the emission-line properties of radio galaxies at different redshifts, we can study the interplay between active galactic nuclei and their host galaxies as a function of cosmic epoch. The emission-line nebulae provide both a direct probe of the conditions in the interstellar medium of the host, and an indirect probe of the central source of ionizing radiation. The most spectacular emission-line nebulae in these systems can have luminosities above 10^{37} W, sizes of over 100 kpc, and a strong alignment with the radio axis (McCarthy et al. 1987, Baum et al. 1988, Chambers, Miley & van Breugel 1987,1988, McCarthy & van Breugel 1989, and McCarthy et al. 1995).

The emission line nebulae of high redshift radio galaxies are usually studied via the redshifted Ly α line, which can, in principle, be strongly affected by extinction from even a small amount of dust due to resonant scattering. Although most powerful radio galaxies are bright in Ly α (McCarthy & Lawrence 1993), dust and density stratification in the interstellar gas can have a strong effect on the flux and spatial distribution of the line-emitting material seen in the rest frame ultraviolet. The distorted morphologies (Heckman et al. 1986), large infrared luminosities (Golombek, Miley & Neugebauer 1988), and molecular gas contents (Mirabel, Sanders & Kazes 1989; Mazzarella et al. 1993; Evans 1996) of radio galaxies at low-redshift imply a great deal of dust in these systems. It might be expected therefore, that these conditions exist in some high-redshift radio galaxies as well. For example, 4C +41.17 and 8C1435+63 have been found to have sub-mm flux densities consistent with thermal dust emission (Dunlop et al. 1994, Ivison 1996). Also, recent observations of 4C +05.41 (Dey, Spinrad & Dickinson 1995) and TX0211–122 (van Ojik et al. 1994) have provided data in support of models of dusty systems at high redshift.

If high-redshift radio galaxies are dusty like many of their low redshift counterparts, the nebular properties (e.g. sizes, morphologies and luminosities) gleaned from observations of Ly α might be misleading. Besides dust, associated HI absorption systems can apparently have a strong effect on the Ly α properties of high redshift galaxies (van Ojik et al. 1997) as well. However, by combining Ly α and H α and/or [OIII] images of high redshift radio galaxies it might be possible to construct extinction and/or ionization “maps” of the emission-line nebulae. Since much work has been devoted to the study of the optical emission-line nebulae of low redshift galaxies, near infrared images of radio galaxies at $z > 2$ made through narrow-band filters provide a means for direct comparison in the same rest-frame emission features.

Besides being valuable laboratories in which to study the interplay between relativistic radio plasmas and dense, galactic gas, the stellar properties of high-redshift radio galaxies can offer significant leverage on cosmological parameters. Powerful radio sources at $z > 2 - 3$ are likely to reside within massive galaxies which may still be growing via accretion at a time when the Universe was only 10% – 20% of its current age. Thus, the host galaxies of high redshift AGN may provide a glimpse of the formation and build up of the most massive stellar systems seen around us today. Large galaxies at high redshift may also mark the locations of young clusters whose cannibalised members form the stellar building blocks of the central host, and provide gas to stoke the engine of the radio source.

The combination of narrow-band filters, sensitive, large format infrared arrays, and large aperture telescopes naturally lends itself to searches for high redshift active, or star forming galaxies in young clusters (see Bunker et al. 1995, Mannucci & Beckwith 1995, and Thompson, Mannucci & Beckwith 1996). While clustering around powerful radio galaxies at $z \sim 0.5$ seems to be enhanced compared to lower redshifts (Hill & Lilly 1991), the clustering properties of radio galaxies at $z > 1$ are largely unknown, with a pair of notable exceptions. Narrow-band Ly α imaging and follow-up spectroscopy of the field around the $z = 3.14$ radio galaxy MRC0316-257 confirm the existence of two faint galaxies at the same redshift as the radio source (Le Fevre, et al. 1997). In addition, Pascarella et al. (1996) have discovered 10 – 20 objects in the field of the

$z = 2.39$ radio galaxy 53W002 via HST Ly α imaging and follow-up spectroscopy. Thus at least two groups or clusters are known around powerful radio galaxies at $z > 2$.

As part of a program to study the continuum and emission-line properties of high redshift AGN in the near-infrared, we have imaged the $z = 3.594$ radio galaxy, 4C +19.71 (MG 2141+19) using the W.M. Keck Telescope. 4C +19.71 is a double-lobed, steep-spectrum, FRII (Fanaroff and Riley class II - Fanaroff & Riley 1974) radio source (Rottgering et al. 1994). The two radio lobes are separated by $8.1''$ at a position angle on the sky of 176° . The integrated flux density in the lobes at 1465 MHz is $S_{1465} \sim 3 \times 10^{-27} \text{ W m}^{-2} \text{ Hz}^{-1}$, implying an emitted monochromatic power at a rest frequency of 6.73 GHz of approximately $10^{28} \text{ W Hz}^{-1}$. The galaxy associated with 4C +19.71 has been imaged previously in the K-band by Eales & Rawlings (1996) and was shown to have two faint components separated by approximately $4''$. The redshift of the galaxy is $z = 3.594$ (Spinrad et al. 1993). Eales & Rawlings present a K-band spectrum showing a weak feature at $\sim 2.3\mu\text{m}$, identified as the [OIII] 5007Å line, having a flux of $2.2 \pm 0.4 \times 10^{-18} \text{ W m}^{-2}$. Here, we present both broad-band K and narrow-band $2.3\mu\text{m}$ images of 4C +19.71, which reveal a resolved central component at K, and a large, asymmetric emission line nebula aligned along the radio axis. The total [OIII] 5007Å emission-line luminosity of the nebula is about $3 \times 10^{37} \text{ W}$, and the linear extent along the major axis is 74 kpc.

In the following sections we describe the observations and present the imaging results. In section 4 we relate the nebular properties of 4C +19.71 to other powerful radio galaxies, estimate the rest frame blue continuum luminosity of 4C +19.71, and discuss the limits on clustering around the radio galaxy probed by our narrow-band imaging.

Throughout this paper we adopt $H_0 = 75 \text{ km s}^{-1} \text{ Mpc}^{-1}$ and $q_0 = 0$, so that at the redshift of 4C +19.71, 9.3 kpc projects to $1''$ on the sky.

2. Observations and Data Reduction

Observations of 4C +19.71 were made at the W.M. Keck Observatory on the night of 5 September 1996 with the Near Infrared Camera (Matthews & Soifer 1994). The radio galaxy was imaged through a standard K-band, 2.0-2.45 μm , filter as well as through a narrow, 2.284-2.311 μm , filter designed to sample the CO stellar absorption feature in zero redshift galaxies. At a redshift of $z = 3.594$, the [OIII] 5007 \AA emission-line feature, but not the 4959 \AA feature, falls in the bandpass of the narrow-band filter. The plate scale of the 256x256 InSb array is 0.15'' per pixel. The total integration time through the K filter was 1080 seconds while the total integration time through the narrow band filter was 2700 seconds. In each case, individual images of 60 and 150 seconds duration, respectively, were taken with the galaxy moved by about 10'' on the array between successive exposures. An offset guider employing a visual wavelength CCD was used to guide the telescope. A nearby star (referred to as star A in Fig. 1) was visible in each exposure and used to register the individual frames. The conditions were photometric during the observations, and UKIRT faint standard stars (Casali & Hawarden 1992) provided the flux calibration. The seeing during the observations was 0.4'' – 0.5'' full width at half maximum (FWHM). To remove time-variable fluctuations in illumination, separate sky and normalized flat-field frames were created from the data for each three images, by taking the median of the nearest 7-9 frames. After being trimmed to a size of 251 \times 251 pixels, the individual data frame are thus sky subtracted and flat fielded and are shifted to a common dc level after known bad pixels are flagged. These processed images are then aligned, using integer pixel shifts, and combined using a clipped mean algorithm.

3. Results

Near infrared K-band images of 4C +19.71 are presented in Figs. 1 and 2. Fig. 1 is an image of the 49'' \times 49'' field surrounding the radio galaxy. The FWHM of a stellar point source in Fig. 1 is 3.3 pixels, or 0.5''. All confidently detected sources, both resolved and unresolved, are labelled

in Fig. 1. The K-band magnitudes of these sources are given in Table 1. We estimate a point source (3σ) detection limit of $K \sim 22.5$ mag in the final mosaic.

The radio galaxy 4C +19.71 has two obvious $2.2\mu\text{m}$ components (see Fig 2 for an expanded picture) labelled as “a” and “b” after Eales & Rawlings (1996). Both components are resolved in our image, and component “a” has a faint extension to the south. The magnitudes of components “a” and “b”, as measured through $2.0''$ diameter circular apertures, are $K = 20.14 \pm 0.05$ mag and $K = 21.41 \pm 0.16$ mag, respectively. The total K magnitude of 4C +19.71 as measured from our data through a rectangular aperture of $2'' \times 10''$, oriented north-south, centered on component “a”, and excluding G6, is $K = 18.92 \pm 0.04$ mag. In Table 1, the K-band magnitudes of all the sources identified in Figure 1 are given, as are the positions relative to component “a” of 4C +19.71.

In Fig. 2 we show the central $\sim 20''$ region of the 4C +19.71 field imaged through both the broad-band K and narrow-band $2.3\mu\text{m}$ filters. The difference in the appearance of 4C +19.71 in the broad and narrow-band images is striking. This difference is due to strong, redshifted [OIII] 5007\AA emission. The [OIII] emission line nebula of 4C +19.71 is extended for over $8''$, or about 74 kpc, and is highly elongated in the north-south direction, with an axial ratio of about 8:1. South of component “a” the nebula is nearly linear with a flaring at the end. Note that component “a” in Fig. 2 actually appears to be either double, or have a core plus “jet” morphology. The position angle between the primary and secondary (fainter) parts of component “a” (“a₁” and “a₂” respectively) is approximately 160° , and it thus does not match the position angle of the nebula as a whole. North of component “a” the nebula is much more diffuse, possibly curving to the west at the location of component “b”. The length of the nebula is comparable to the separation of the radio lobes mapped by Rottgering et al. (1994) and the overall position angle of the [OIII] emission is the same as the position angle of the radio lobes on the sky is $176^\circ \pm 3^\circ$. Eales & Rawlings (1996) also note that the [OIII] emission appears extended to the north in their K-band spectrum.

From these data the 4C +19.71 nebula has an [OIII] 5007\AA emission-line flux measured within a $2'' \times 10''$ rectangular aperture of 1.54×10^{-18} W m⁻², corresponding to a 5007\AA line

luminosity of about 3×10^{37} W. Eales & Rawlings (1996) measure an [OIII] 5007Å line flux of $\sim 10^{-18}$ W m⁻² through a 3.1'' × 3.1'' slit, and $\sim 2 \times 10^{-18}$ W m⁻² through a 3.1'' × 12.4'' wide slit, oriented at a position angle of 162°. By comparing the line flux to the total emission measured through the K-band filter, we estimate that the 5007Å line alone comprises approximately 34% of the broad K-band flux. The rest frame equivalent width of the 5007Å line, when averaged over the entire nebula, is 560 ± 58 Å. Note that the total [OIII] line contribution to the measured K-band flux is about 45%.

The nature of the K \sim 19.8 mag source (G6) located approximately 2.1'' northwest of component “b” is unknown. It’s proximity to the radio source argues that it may be associated, especially since it lies along what appears to be a bend in the emission-line nebula beyond component “b”. However, G6 has no discernible excess of flux in the narrow band filter, indicating that there is no strong [OIII] emission from this source. Given its lack of a narrow-band color excess and a K= 19.78 ± 0.05 mag, we calculate a line flux limit of about 3×10^{-20} W m⁻² from G6. If G6 is at the redshift of 4C +19.71, this corresponds to a limit on its [OIII] line luminosity of about 7×10^{35} W, or about 2% of that measured for the radio galaxy nebula as a whole.

In Fig. 3 we present a plot of the difference between the broad and narrow-band magnitudes (the color “excess”) versus the broad-band magnitude for the objects in the 4C +19.71 field. All of the sources identified in Fig. 1 and Table 1 are plotted here, except for G8 and obj 12, which have been excluded because the uncertainties in their narrow-band magnitudes are larger than 50%. The large narrow-band color excess of 4C +19.71 is obvious in Fig. 3. We have indicated two points for 4C +19.71 in Fig. 3 - components “a” and “b” as defined above. The different locations of the two points in Fig. 3 reflect the variation of the [OIII] 5007Å emission-line equivalent width along the extent of the 4C +19.71 nebula, in the sense that the equivalent width of the nebula is larger away from the galaxy nucleus. This simply reflects the fact that there is very little continuum light in the galaxy (at least to the limits of this image) at large radii along the nebular axis.

Besides 4C +19.71 itself, there are three sources with an apparent narrow-band excess at

the 3σ level or above. These are the bright resolved sources labelled G1 and G2, and the bright, apparently stellar source labelled star B. Sources G1 and G2 have narrow-band excesses at the $3 - 3.5\sigma$ level, while star B has an excess at closer to the 5σ level. Object 10 has a large narrow-band excess (0.41 mag), but the uncertainties are large (± 0.23 mag). The other nine sources plotted in Fig. 3 scatter about the $K-NB = 0.0$ mag line, with a total dispersion of about 0.2 mag. An excess of 0.2 mag corresponds to an $[\text{OIII}] 5007\text{\AA}$ rest frame equivalent width of about 13\AA at the redshift of 4C +19.71.

4. Discussion

Since 4C +19.71 is one of only three galaxies at $z > 3$ to be imaged in an emission line, it is instructive to place the 4C +19.71 nebula within the context of those seen around other powerful radio galaxies. The two largest sets of radio galaxy narrow-band imaging data are those compiled by Baum et al. (1988) and McCarthy, Spinrad & van Breugel (1995). The low redshift ($0.003 < z < 0.48$) 3CR sources imaged by Baum et al. (1988) have visual emission-line luminosities of $2.2 \times 10^{32} - 1.3 \times 10^{36}$ W (median $L \sim 3 \times 10^{34}$ W) and sizes of 1 – 96 kpc (median diameter, $d \sim 10$ kpc). The intermediate redshift ($0.058 < z < 1.847$) 3CR nebulae imaged by McCarthy, Spinrad & van Breugel (1995) have visual emission-line luminosities of $2 \times 10^{33} - 2 \times 10^{37}$ W (median $L \sim 6 \times 10^{35}$ W), corrected to $[\text{OIII}] 5007\text{\AA}$ using emission-line flux ratios of $[\text{OIII}]/\text{H}\alpha + [\text{NII}] = 1$, $[\text{OIII}]/\text{Ly}\alpha = 0.3$, and $[\text{OIII}]/[\text{OII}] = 3$, and sizes of 1 – 213 kpc (median $d \sim 30$ kpc). Five systems in the McCarthy, Spinrad & van Breugel sample (about 15%) at redshifts of $z > 0.5$ have nebulae larger than 100 kpc, as measured down to a surface brightness level of 10^{-20} W m⁻² arcsec⁻². There are nebula found in both data sets with large, elongated features (e.g. 3C 227, 3C 458, 3C 435A), yet none are dominated by a single, high surface brightness, high axial ratio nebulosity as seen in 4C +19.71.

Although the the Baum et al. (1988) and McCarthy et al. (1995) samples are the largest existing narrow-band imaging data sets, most of the objects are at redshifts well below $z \sim 2$. From a sample of steep spectrum 4C radio sources, Chambers et al. (1996a,b) image five galaxies

with $2.348 < z < 2.905$ through narrow-band filters matched to the Ly α line. The Ly α nebulae of these galaxies range from about 25 – 90 kpc in extent, and are generally aligned along the radio axis.

At $z > 3$ there are two systems previously known to possess large, emission-line nebulae. A large (~ 60 kpc), apparently rotating Ly α halo has been imaged around the $z = 3.57$ radio source 4C 03.24 by van Ojik et al. (1997). The Ly α luminosity of the nebula in 4C 03.24 is about 6×10^{37} W. Graham et al. (1994) imaged the [OIII]+H β nebula around the $z = 3.8$ radio galaxy 4C +41.17 by taking the difference between images in a standard K-band and a K $_s$ ($2.0 - 2.3\mu\text{m}$) filter. These authors show that the nebula has an extent of about 15×40 kpc, and that it is oriented along the radio axis. However, unlike 4C +19.71, the 4C +41.17 nebula is wider, and appears to extend beyond the main radio components. Chambers, Miley & van Breugel (1990) showed that 4C +41.17 also has a large Ly α nebula which is similarly extended along the radio axis.

4.1. Relation of [OIII] and Radio Properties of 4C +19.71

4C +19.71 is a double-lobed, FR II radio source with a lobe separation of $8.1''$ at a position angle of 176° . There is no obvious central radio core. The monochromatic power at a rest frequency of 6.76 GHz is approximately 10^{28} W Hz $^{-1}$. The extent of the [OIII] nebula matches the separation of the radio lobes in 4C +19.71, and the overall position angle of the nebula is similar to the position angle of the radio lobes. Although the absolute positioning of the infrared images is uncertain, and the radio map has no strong core, an R-band image of the field covering 10 arcminutes and including six HST guide stars as well as “star A” indicates that to within an uncertainty of $\sim 2''$, the lobes are centered on component “a $_1$ ”. If “a $_1$ ” is the nucleus of the radio galaxy, and also the centroid of the two radio lobes, then the radio lobes are located on the [OIII] image as depicted in Fig. 2. This positioning suggests that a narrow, slightly curving “corridor” of line-emitting gas fills the regions between the galaxy nucleus and the radio lobes. This gas does not extend beyond the radio lobes to a limiting surface brightness of about 2×10^{-20} W m $^{-2}$

arcsec⁻². Note that the position angle between the primary and secondary parts of component “a” is not the same as that of the nebula as a whole or the radio lobe axis. Thus if “a₂” represents a hotspot in the emission line gas caused by the interaction of an inner jet with the interstellar medium of 4C +19.71, a precession of the jet, or a bend caused by the interaction of the jet with an overdense region, may explain the difference in the position angle between the inner and the outer nebula.

The emission-line–to–radio luminosity ratio in 4C +19.71 is entirely consistent with the relation found for other FR II radio sources over a large range in redshift. In Fig. 2 of McCarthy (1993) the luminosity in the [OII] 3727Å line is plotted against the monochromatic radio power at an observed frequency of 1400 MHz. A clear correlation exists over five orders of magnitude in radio and emission-line power. If the [OIII] 5007/[OII] 3727 line flux ratio in 4C +19.71 is 3.0, the [OII] luminosity is about 10³⁷ W. Similarly the radio spectral index of $\alpha = -1.24$ (Rottgering et al. 1994), where $f_\nu \propto \nu^\alpha$, implies a 1400 MHz flux density of $\sim 3 \times 10^{-27}$ W m⁻² Hz⁻¹, and thus a monochromatic power at an emitted frequency of 6.43 GHz of about 1.4×10^{28} W Hz⁻¹. For this radio power, the predicted [OII] luminosity of 4C +19.71 is slightly larger than the average value, yet well within the scatter in the McCarthy plot. If $\alpha = -1.24$ out to an observed frequency of about 300 MHz, the monochromatic power at an emitted frequency of 1400 MHz is closer to 10²⁹ W Hz⁻¹, thus placing 4C +19.71 near the center of the emission-line–radio power correlation. Thus both the morphology and the overall luminosity of the optical emission-line gas and radio plasma in 4C +19.71 suggest a causal link between the relativistic electrons and the 10⁴K ionized gas.

There are a number of possible explanations for the correlation of the optical emission-line gas and the radio plasma in 4C +19.71. This gas could be photoionized by the active nucleus, or ionized by shocks associated with the radio jets responsible for supplying the radio lobes with energetic electrons. The emission-line gas may form a shell or channel around the radio jet as has been seen in the nearby Seyfert galaxy NGC 1068 (Gallimore et al. 1996, Capetti, Macchetto & Lattanzi 1997). Alternatively, the expanding jets could trigger star formation in the host galaxy,

and these hot stars could ionize the surrounding medium. This would indicate a more indirect connection between the radio emission and the optical line-emitting gas. The strong alignment in position angle between the radio lobes and the [OIII] gas, and the similarities in their overall dimensions could be used to argue for any or all of these possibilities. The 560\AA rest frame equivalent width of the [OIII] line is much larger than what is seen in starburst galaxies, yet is comparable to the largest values seen in powerful radio galaxies, being a factor of ~ 2 larger than the “typical” value tabulated by McCarthy (1993). Thus it is unlikely that the bulk of the [OIII] emission is produced by young stars. Longslit, near infrared spectroscopy of the $2.3\mu\text{m}$ spectral region at high spectral resolution could provide a more concrete assessment of the source of ionizing photons through a measurement of the the linewidth and flux ratio of the [OIII] 5007\AA and $\text{H}\beta$ emission lines. In the spectrum presented by Eales & Rawlings (1996) the $\text{H}\beta$ emission-line is undetected, suggesting that the [OIII] $5007/\text{H}\beta$ line flux ratio is greater than 7-10, consistent with a hard source of ionizing photons (Veilleux & Osterbrock 1987).

4.2. Dust and Gas in 4C +19.71

4.2.1. Dust

By comparing the [OIII] 5007\AA emission-line flux reported here with the flux of another emission-line whose ratio to [OIII] is known, we can estimate the amount of reddening towards the ionized gas in 4C +19.71. As pointed out by Dey, Spinrad & Dickinson (1995), the fact that there are only three known dusty, high redshift galaxies implies that these objects are either intrinsically very rare, or they have been systematically missed in surveys due to observational biases. However, since the presence of significant amounts of dust in a high redshift galaxy requires the dust to have been formed at an even earlier epoch, dusty systems at $z > 2$ may imply very early star formation episodes.

Recombination lines are best suited to the task of determining reddening toward the emission-line gas, but pairs of these have not yet been measured in 4C +19.71. However, a

total Ly α flux has been measured in 4C +19.71 to be about 1.1×10^{-18} W m $^{-2}$ (H. Spinrad & M. Dickinson, private communication). Thus the measured [OIII] 5007Å to Ly α line flux ratio, averaged over the entire 4C +19.71 nebula, is ~ 1.4 . We can estimate the amount of reddening toward 4C +19.71, by assuming the intrinsic spectrum is similar to the “average” radio galaxy spectrum compiled by McCarthy (1993). Since powerful radio galaxies typically have [OIII] 5007/Ly α line flux ratios of about 0.3 (McCarthy 1993), the increased ratio measured for 4C +19.71 may indicate the presence of dust. To account for the increase in the [OIII] 5007/Ly α line flux ratio seen here would require a visual extinction of only $A_V \sim 1$ mag. With an $l^{\text{II}} = 75^\circ$ and a $b^{\text{II}} = -30^\circ$, the Galactic color excess towards 4C +19.71 is $E(B-V) \sim 0.04 - 0.05$ mag (Burstein & Heiles 1982), implying an $A_V \sim 0.12 - 0.16$ mag, negligible in comparison to the amount of extinction required if the intrinsic [OIII] 5007/Ly α line flux ratio is 0.3. An $A_V \sim 1$ mag is not very large, yet it implies a significant mass of associated HI gas, if the dust is spread out over the entire nebula. If $A_V = 5.3 N_{\text{H}}/10^{22}$ mag (Bohlin, Savage & Drake 1978), the HI column density toward the emission-line gas in 4C +19.71 is about 2×10^{21} cm $^{-2}$. If this gas is spread out over a projected surface area of $8'' \times 1''$ or 691 kpc 2 , the implied HI gas mass is about $10^{10} M_\odot$. An atomic-to-molecular gas ratio similar to the Galaxy thus implies a similarly large mass of H $_2$ (Young & Scoville 1991). Of course, if Ly α is resonantly scattered throughout the nebula, a very small amount of dust could be responsible for the depleted line flux, in turn implying much less HI, and by inference, much less molecular gas in 4C +19.71.

Under dusty conditions we would expect the nebula as seen in Ly α to have a different morphology and perhaps be much smaller in extent than the nebula as seen in [OIII]. However, images of 4C +19.71 in the Ly α line (L. Maxfield & M. Dickinson, private communication) suggest the nebula has a projected size which is at least as large as the [OIII] nebula imaged here. Dust which is not uniformly distributed over the face of the galaxy, perhaps in a dusty disk or torus around the nucleus, could serve to remove much of the rest frame UV from our line of sight yet still allow ionizing photons to escape along the radio jet axis, as in the standard AGN unification model (e.g. Antonucci 1993). Alternatively the “average” extinction we have calculated may be dominated by small, dense clumps of dust and gas scattered throughout the nebula.

Although the average visual extinction required to bring the observed 4C +19.71 [OIII] 5007/Ly α line flux ratio in line with most other powerful radio galaxies is small, it is predicated upon the assumption that the nebula is photoionized. In general this is a good assumption, since photoionization models can reproduce the emission-line flux ratios measured in many radio galaxies (McCarthy 1993). However, if there are significant dynamical ionization processes such as shocks, the intrinsic [OIII] 5007/Ly α flux ratio can be as low as 0.04 (Dopita & Sutherland 1995). In this case the required visual extinction to the 4C +19.71 nebula would be $A_V > 2$ mag, using the measured [OIII] 5007 \AA and Ly α line fluxes.

4.2.2. Ionized Gas

The size of the 4C +19.71 [OIII] nebula implies a distribution of potentially metal-rich gas on galactic scales. To determine the mass of ionized gas around 4C +19.71 we must know either the gas density, or the volume and volume filling factor of the nebula. For a collisionally excited transition such as the [OIII] 5007 \AA line, the cooling rate per unit volume in the low density limit is $N_2 A_{21} h \nu_{21} = n_e N_1 q_{12} h \nu_{21}$ (Osterbrock 1974), where N_2 is the number density of O^{++} atoms in the excited state, N_1 is the number density of O^{++} atoms in the lower state, A_{21} is the radiative transition probability, and q_{12} is the collisional excitation rate. For the [OIII] 5007 \AA line, $A_{21} h \nu_{21} = 7.5 \times 10^{-14}$ erg s $^{-1}$ and $q_{12} = 4.1 \times 10^{-9}$ cm $^{-3}$ s, for $T = 10^4$ K (Osterbrock). The mass of O^{++} can then be written as,

$$M_{\text{OIII}} = 8.7 \times 10^7 L_{44}^{5007} n_e^{-1} M_{\odot} \quad (1)$$

where L_{44}^{5007} is the luminosity in the 5007 \AA line in units of 10^{44} erg s $^{-1}$. Although we do not know the ionization state of the gas from a single measurement of [OIII], if the ratio of O^{++}/O in the nebula is about 0.3 (as it is in Cygnus A - Osterbrock), the total mass of ionized hydrogen is,

$$M = 1.4 \times 10^{11} (n_e Z)^{-1} M_{\odot}, \quad (2)$$

where Z is the O/H ratio of the nebular gas in solar units. Thus if $n_e = 10^2 \text{ cm}^{-3}$ and $Z = 1$, the total mass of ionized gas in the 4C +19.71 is about $10^9 M_\odot$. This is comparable to the most massive nebulae seen around low redshift radio galaxies in the light of visual emission-lines such as [OIII] 5007Å and $\text{H}\alpha + [\text{NII}]$ (Baum & Heckman 1989).

By combining these mass estimates with those made from a recombination line such as $\text{Ly}\alpha$ or $\text{H}\alpha$, we can solve for the O/H ratio, given assumptions about the volume and the volume filling factor of the gas. For pure case B recombination, the mass of ionized gas in the nebula as determined from the luminosity in the $\text{Ly}\alpha$ line is $M = 1.3 \times 10^8 (f_5 V_{68} L_{44}^{\text{Ly}\alpha})^{1/2} M_\odot$ or $M = 2.1 \times 10^{10} L_{44}^{\text{Ly}\alpha} n_e^{-1} M_\odot$, where f_5 is the volume filling factor in units of 10^{-5} , V_{68} is the volume of the nebula in units of 10^{68} cm^3 , and $L_{44}^{\text{Ly}\alpha}$ is the $\text{Ly}\alpha$ line luminosity in units of $10^{44} \text{ erg s}^{-1}$. From measurements of the gas density in the optical line-emitting nebula of radio galaxies at low redshift, typical volume filling factors of $10^{-4} - 10^{-5}$ have been derived (Heckman, van Breugel & Miley 1984). Assuming cylindrical symmetry, we estimate the volume of the nebula in 4C +19.71 to be about $1.5 \times 10^{68} \text{ cm}^3$. Thus, if $f_5 = 1$, $V_{68} = 1.5$, and $L_{44}^{\text{Ly}\alpha} = 2.1$ (H. Spinrad, private communication), $M = 2.3 \times 10^8 M_\odot$, and $n_e = 190 \text{ cm}^{-3}$. This assumes that the $\text{Ly}\alpha$ emitting nebula is of similar volume as the [OIII] nebula mapped here, and that $A_V = 0 \text{ mag}$. Note that if $A_V = 1 \text{ mag}$ for the nebula and $f_5 = 1$, the implied mass is closer to $10^9 M_\odot$ and the electron density is about 675 cm^{-3} .

Equating the masses derived from both the [OIII] and the $\text{Ly}\alpha$ lines suggests that $Z \sim 3$ for the nebular gas if $A_V = 0 \text{ mag}$. A galaxy at $z = 3.6$ might be expected to be in the early stages of its evolution and thus have low overall metallicity. Indeed, many damped $\text{Ly}\alpha$ absorption line systems at high redshifts appear to have very low metallicities ranging from $10^{-3} - 10^{-2}$ of the solar value (e.g. Lu et al. 1996), consistent with hierarchical models of structure formation (e.g. Rauch, Haehnelt & Steinmetz 1997, Hellsten et al. 1997). However, AGN emission lines typically imply solar or above metallicities over a large range in redshift. In high redshift quasars, this has been taken to imply early, and vigorous star formation pre-dating the AGN phase (Hamann & Ferland 1992,1993). If the [OIII] nebular gas in 4C +19.71 is metal-rich, it must have been processed

through stars before the observed epoch. At $z = 3.6$, the maximum age of a stellar population is about 2 Gyr. This maximum age is closer to 5×10^8 yrs if the formation redshift is $z \sim 5$. By comparison, values of $Z \sim 3$ are reproduced in the galactic chemical evolution models of Matteucci & Padovani (1993) for massive galaxies at ages of only about 0.3 Gyr for Salpeter (or flatter) IMF slopes. Flatter IMF spectral indices can generate O/H ratios of a few times solar after only 0.1 Gyr. While O/H ratios above solar are easily explained in terms of an early starburst for 4C +19.71, an $A_V = 1$ mag for the nebula would imply an O/H ratio of about 0.7 solar, for values of the filling factor and nebular volume given above. Since extinctions much larger than $A_V = 1$ mag probably do not apply to the 4C +19.71 nebula overall, unless the intrinsic [OIII] 5007Å–to–Ly α line flux ratio is significantly different than what is seen in other powerful radio galaxies, it is unlikely that the emission-line gas has a metallicity far below solar. However, another uncertainty in this calculation is the temperature of the line-emitting gas. Lower metallicities imply hotter temperatures, stronger [OIII] emission, and lower oxygen masses. If $T \sim 2 \times 10^4$ K, the oxygen mass is about 36% of the value estimated above, and the O/H ratio closer to solar for an $A_V = 0$ mag. Thus, while early enrichment by a previous ($z > 3.6$) episode of star formation is consistent with the data, the derivation of the metallicity of the gas is highly uncertain and values of the O/H ratio from a few tenths to a few times solar are possible.

4.2.3. Pressure Balance in the 4C +19.71 Radio Lobes

The radio properties of 4C +19.71 (under the assumption of pressure balance between the radio plasma and the gas), can also be used to estimate the mass of the nebula. Following Miley (1981), we can write the magnetic field strength, under energy equipartition, as $B \sim 1.5 \times 10^{-3} [F_o / \theta^2 S]^{2/7}$ G, where F_o is the measured flux density of the source in Jy, θ^2 is the surface area of the lobe in arcsec², and S is the path length through the source in kpc. If the radio lobes have a spectral index of $\alpha = -1.24$, the volume filling factor of the synchrotron emitting plasma is unity, and the radio lobes occupy spheres of 1'' (about 9 kpc) diameter, each with a flux density of 0.15 Jy at 1.465 GHz, the minimum energy condition implies a magnetic field of $\sim 5 \times 10^{-4}$ G. If the radio

lobes are confined by static, thermal pressure from a gas at 10^4K , a gas density of more than $6 \times 10^{-21} \text{ gm cm}^{-3}$ is implied. However, if the lobes are instead confined by ram pressure and we use the axial ratio of the emission line gas (approximately 5:1 from core to lobe) and a typical lobe advance speed of $v \sim 0.01c$ (Readhead et al. 1996) we can estimate a lateral velocity of $v \sim 0.002c$. The implied gas density is then greater than about $2 \times 10^{-25} \text{ gm cm}^{-3}$. If the volume filling factor is 10^{-5} , the densities derived from the pressure equilibrium arguments imply gas masses of about $5 \times 10^9 M_\odot$ and $4 \times 10^6 M_\odot$, respectively, if the densities are representative of the entire nebula.

4.3. Continuum Luminosity of 4C +19.71

In a $2'' \times 10''$ beam, the [OIII] 5007Å line contributes approximately 34% of the total flux in the K band, and the observed $2.2\mu\text{m}$ continuum of 4C +19.71 therefore has $K \sim 19.6$ mag, if the [OIII] 4959Å line has 1/3 the flux of the 5007Å line. We have not subtracted a contribution from $H\beta$ to derive the continuum magnitude, but this is likely to be relatively small, perhaps 10% the flux of the 5007Å line (Eales & Rawlings 1996). In order to compare the continuum magnitude to that expected from “normal” galaxies at $z \sim 3.6$, we employ the luminosity function of Mobasher, et al. (1993), such that an E/S0 galaxy has a characteristic absolute magnitude, $M_B^* = -20.24$ mag, following Schechter (1976). Combining this characteristic absolute magnitude with the spectral energy distributions of Coleman, Wu & Weedman (1980), we estimate that the apparent K-band magnitude of an L^* elliptical galaxy at $z \sim 3.6$ is $K \sim 23.5$ mag. Thus, if the rest frame visual continuum light from 4C +19.71 is produced by stars, it implies a $40L^*$ host galaxy. This is extremely luminous, yet the host galaxies of some radio loud quasars (Heckman et al. 1991; Lehnert et al. 1992; Armus et al. 1997) as well as radio galaxies (Eales & Rawlings 1993, 1996; Evans et al. 1996) at redshifts of $z \sim 2 - 3$ appear to have rest frame visual luminosities in this range. Although significant fading (by 2-4 magnitudes in the rest frame visual) would be required for these systems to evolve into galaxies resembling even the brightest cluster ellipticals at the present epoch, this amount of fading can be accommodated by the postburst models of Chambers & Charlot (1990) and Charlot & Bruzual (1991). Of course, if much of the continuum emission

at these wavelengths in 4C +19.71 is scattered AGN light, the host galaxy may be significantly fainter than $K \sim 19.6$ mag, and the amount of fading required would be correspondingly lower.

4.4. Clustering

Although the goal of this paper is not to search for young clusters or “protogalaxies”, it is worthwhile to explore the possibility of clustering around 4C +19.71. At $z = 3.594$ an L^* spiral galaxy has $K \sim 23.7$ mag. Since the 3σ point source detection limit our K-band image is $K \sim 22.5$ mag, objects at the redshift of 4C +19.71 would be difficult to detect in the continuum unless they were at least one magnitude brighter than an L^* galaxy. However, strong sources of line emission at specific redshifts ($z \sim 3.6$ for [OIII] or $z \sim 2.5$ for $H\alpha$) could be detected through their excess light at $2.3\mu\text{m}$ as measured with the narrow band filter.

Besides 4C +19.71 itself, there are three sources with an apparent narrow-band excess at the 3σ level or above. The bright sources G1 ($K \sim 16.0$ mag) and G2 ($K \sim 15.4$ mag) are well resolved, and it is likely they are foreground to 4C +19.71. Infrared lines such as $\text{Br}\gamma$ at $z \sim 0.062$, H_2 (1-0 S(1)) at $z \sim 0.084$, HeI at $z \sim 0.118$, or $\text{Pa}\alpha$ at $z \sim 0.227$ are possibilities for the source of the excess in G1 and G2. The third source showing a significant ($\sim 5\sigma$) narrow-band flux excess is star B. This source is intriguing since it is unresolved in the K-band image, but slightly elongated in the narrow-band $2.3\mu\text{m}$ image. The true nature of this source is unknown, but its brightness ($K \sim 16.7$ mag) argues against it being at a redshift of $z = 3.6$. The other ten sources plotted in Fig. 3 scatter about the $K\text{-NB} = 0.0$ mag line, with a total dispersion of about 0.2 mag, except for obj 10 which has a large uncertainty in its narrow-band excess. Since an excess of 0.3 mag corresponds to a rest frame equivalent width of about 10\AA at the redshift of 4C +19.71, none of the remaining sources can be emission-line objects at the redshift of 4C +19.71 with [OIII] emission-line equivalent widths of more than about 2% of that measured for 4C +19.71. A source present at the 3σ level in both the K-band and the narrow-band $2.3\mu\text{m}$ images would have an implied [OIII] line flux of $\sim 2 \times 10^{-20} \text{ W m}^{-2}$. The limiting line flux for obj 12 (the faintest narrow-band source in the central part of Fig. 1) is approximately $10^{-20} \text{ W m}^{-2}$. If [OIII]/ $H\alpha \sim 1$,

then this flux limit corresponds to an $H\alpha$ luminosity of about 2×10^{35} W, and a star formation rate limit of about $17 M_{\odot} \text{ yr}^{-1}$ (Kennicutt 1983). The co-moving volume covered by our image is 212 Mpc^3 at $z = 3.6$ (for $H_0 = 75 \text{ km s}^{-1} \text{ Mpc}^{-1}$ and $q_0 = 0$). Thus the space density of objects with $K < 22.5$ mag and $[\text{OIII}] 5007\text{\AA}$ emission-line equivalent widths of more than about 10\AA in the vicinity of 4C +19.71 is less than $5 \times 10^{-3} \text{ Mpc}^{-3}$. Deeper images, at K and in the $2.3\mu\text{m}$ filter, would be required to place limits on L^* or moderately star-forming galaxies around 4C +19.71

5. Summary

Using a broad-band K and narrow-band $2.3\mu\text{m}$ filter, we have observed the $z = 3.594$ radio galaxy 4C +19.71 with the Near Infrared Camera on the W.M. Keck Telescope. These imaging data have allowed us to determine the following properties of the emission-line nebula in this high redshift, powerful radio galaxy:

(1) The $[\text{OIII}]$ nebula has an extent of about 74×9 kpc, and is very narrow with some flaring and bending at the ends. The total luminosity of the nebula is $L_{5007} \sim 3 \times 10^{37}$ W. The fraction of the light that is contributed by the 5007\AA line to the total K-band flux is about 34%.

(2) The length of the $[\text{OIII}]$ nebula is nearly identical to the separation of the two radio lobes mapped at 1465 MHz by Rottgering, et al. (1994), and the position angle of the nebula is similar to that of the radio emission. 4C +19.71 falls on the emission-line vs. radio power correlation found for other powerful radio galaxies at low and high redshifts. Taken together, these facts suggest a direct link between the relativistic electrons and the 10^4K gas in 4C +19.71.

(3) The ratio of the $[\text{OIII}] 5007\text{\AA}$ line luminosity to the total $\text{Ly}\alpha$ line luminosity (H. Spinrad and L. Maxfield, private communication) is ~ 1.4 , larger by a factor of about 4 – 5 than is typically seen in the spectra of powerful radio galaxies (McCarthy 1993). This may indicate the presence of dust in 4C +19.71, or an enhancement in the nebular O/H ratio. The nebula-averaged extinction required to produce the observed $[\text{OIII}]$ -to- $\text{Ly}\alpha$ line flux ratio is only $A_V \sim 1$ mag if the intrinsic ratio is equal to the average value. If resonant scattering of the $\text{Ly}\alpha$ line is not severe, this

extinction implies an HI mass of $10^9 - 10^{10} M_{\odot}$, depending upon the distribution of the obscuring dust.

(4) We derive an ionized gas mass of $2 \times 10^8 - 10^9 M_{\odot}$ from the [OIII] and Ly α emission-line luminosities. The O/H ratio in the nebula is at least a few tenths solar, and may be as high as a factor of three above solar. The latter would argue for a starburst at $z > 3.6$ in 4C +19.71. The gas masses derived by requiring that the radio lobes be either in thermal pressure or ram pressure equilibrium with the 10^4K gas are $5 \times 10^9 M_{\odot}$ and $4 \times 10^6 M_{\odot}$, respectively.

(5) The continuum magnitude of 4C +19.71 is $K \sim 19.6$ mag. At $z = 3.594$, this corresponds to a $40L^*$ E/S0 galaxy. Although the fraction of the continuum light that is non-stellar in origin is not known, this value for the continuum flux places 4C +19.71 along the K-z relation found for radio loud quasars and radio galaxies.

(6) There are three objects, besides 4C +19.71, which have a flux excess in the narrow band filter. Two of these are bright ($K \sim 15.4 - 16.0$ mag) galaxies which are likely to be at low redshifts. The nature of the third object is unknown, but its brightness ($K \sim 16.7$ mag) also argues for a similarly low redshift. There are no candidate emission-line objects at the redshift of 4C +19.71 having [OIII] rest frame equivalent width of more than about 2% of the radio galaxy itself within a co-moving volume of 212 Mpc^3 . Thus the space density of objects with [OIII] emission-line luminosities of $2 - 3 \times 10^{35} \text{ W}$ and rest frame blue luminosities greater than $3L^*$ around 4C +19.71 is less than about $5 \times 10^{-3} \text{ Mpc}^{-3}$.

The W.M. Keck Observatory is operated as a scientific partnership between the California Institute of Technology and the University of California. We thank the entire Keck staff, especially Wendy Harrison, for making these observations possible. In addition, we thank David Hogg, Matt Lehnert, Pat McCarthy, and Tony Readhead for many helpful discussions. Hy Spinrad and Leslie Maxfield were kind enough to make their unpublished visual data available to us, and we thank them for that. The comments of an anonymous referee are also appreciated. Infrared astrophysics at Caltech is supported by grants from NASA. This research has made use of the NASA/IPAC

Extragalactic Database which is operated by the Jet Propulsion Laboratory, Caltech, under contract with NASA.

REFERENCES

- Armus, L., Neugebauer, G., Lehnert, M.D., & Matthews, K. 1997, MNRAS, 289, 621.
- Baum, S.A., Heckman, T.M., Bridle, A., van Breugel, W., & Miley, G.K. 1988, ApJS, 68, 643.
- Baum, S.A. & Heckman, T.M. 1989, ApJ, 336, 681.
- Bohlin, R.C., Savage, B.D., & Drake, J.F. 1978, ApJ, 224, 132.
- Bunker, A.J., Warren, S.J., Hewett, P.C., & Clemens, D.L. 1995, MNRAS, 273, 513.
- Burstein, D., & Heiles, C. 1982, AJ, 87, 1165.
- Capetti, A., Macchetto, F.D., & Lattanzi, M.G. 1997, ApJ, 476, L67.
- Chambers, K.C., & Charlot, S. 1990, ApJ, 348, L1.
- Chambers, K.C., Miley, G.K., & van Breguel, W.J.M. 1987, Nature, 329, 604.
- Chambers, K.C., Miley, G.K., & van Breguel, W.J.M. 1988, ApJ, 327, L47.
- Chambers, K.C., Miley, G.K., & van Breguel, W.J.M. 1990, ApJ, 363, 21.
- Chambers, K.C., Miley, G.K., van Breugel, W.J.M., & Huang, J.-S. 1996, ApJS, 106, 215.
- Chambers, K.C., Miley, G.K., van Breugel, W.J.M., Bremer, M.A.R., Huang, J.-S., & Trentham, N.A. 1996, ApJS, 106, 247.
- Charlot, S., & Bruzual A., G. 1991, ApJ, 367, 126.
- Coleman, G. D., Wu, C-C. & Weedman, D. W. 1980, ApJS, 43, 393
- Dey, A., Spinrad, H., & Dickinson, M. 1995, ApJ, 440, 515.
- Dopita, M.A. & Sutherland R.S. 1995, ApJ, 455, 468.
- Dunlop, J. S. Hughes, D. H., Rawlings, S., Eales, S., & Ward, M. J. 1994, Nature, 370, 347

- Eales, S.A., & Rawlings, S. 1996, ApJ, 460, 68.
- Evans, A.S., Sanders, D.B., Mazzarella, J.M., Solomon, P.M., Downes, D., & Radford, S.J.E. 1996, ApJ, 457, 658.
- Evans, A.S. 1996 Ph.D. Thesis, University of Hawaii.
- Fanaroff, B.L., & Riley, F.M. 1974, MNRAS, 167, 31P.
- Gallimore, J.F., Baum, S.A., & O’Dea, C.P. 1996, ApJ, 458, 136.
- Golombek, D., Miley G.K. & Negebauer, G. 1988, AJ, 95, 26.
- Graham, J.R., Matthews, K., Soifer, B.T., Nelson, J.E., Harrison, W., Jernigan, J.G., Lin, S., Neugebauer, G., Smith, G., & Ziomkowski, C. 1994, ApJ, 420, L5.
- Hamann, F. & Ferland, G. 1992, ApJ, 391, L53.
- Hamann, F. & Ferland, G. 1993, ApJ, 418, 11.
- Heckman, T. M., Smith, E. P., Baum, S. A., van Breugel, W. J. M., Miley, G. K., Illingworth, G. D., Bothun, G. D., & Balick, B. 1986, ApJ, 311, 526
- Heckman, T.M., Lehnert, M.D., Miley, G.K., & van Breugel, W. 1991, ApJ, 381, 373.
- Hellsten, U., Dave, R., Hernquist, L., Weindberg, D.H. & Katz, N. 1997, ApJ, submitted.
- Hill, G.J., & Lilly, S.J. 1991, ApJ, 367, 1.
- Ivison, R. J. 1995, MNRAS, 275, L33
- Kellerman, K.I., Sramek, R.A., Schmidt, M., Schaffer, D.B., & Green, R.F. 1989, AJ, 98, 1195
- Kennicutt, R.C. 1983, ApJ, 272, 54.
- Lacy, M., et al. 1994, MNRAS, 271, 504.

- Le Fevre, O., Deltorn, J.M., Crampton, D., & Dickinson M. 1997, ApJin press.
- Lehnert, M.D., Heckman, T.M., Chambers, K.C., & Miley, G.K. 1992, ApJ,393,68.
- Lu, L., Sargent, W.L.W., Barlow, T.A., Churchill, C.W. & Vogt, S. 1996, ApJS, 107, 475.
- McCarthy, P.J., Spinrad, H., Djorgovski, S., Strauss, M.A., van Breugel, W., & Liebert, J. 1987, ApJ, 319, L39.
- McCarthy, P.J., van Breugel, W., Spinrad, H., & Djorgovski, S. 1987, ApJ, 321, L29.
- McCarthy, P.J., Spinrad, H., van Breugel, W., Liebert, J., Dickinson, M., Djorgovski, S., & Eisenhardt, P. 1990, ApJ, 365, 487.
- McCarthy, P.J. 1993, ARA&A, 31, 639.
- McCarthy, P.J., Spinrad, H., & van Breugel, W. 1995, ApJS, 99, 27.
- Mannucci, F. & Beckwith, S.V.W. 1995, ApJ, 442, 569.
- Matteucci, F., & Padovani, P. 1993, ApJ, 419, 485.
- Mazzarella, J.M., Graham, J.R., Sanders, D.B., & Djorgovski, S. 1993, ApJ, 409, 170.
- Miley, G.K. 1981, ARA&A, 18, 165.
- Mirabel, I.F., Sanders, D.B., & Kazes, I. 1989, ApJ, 340, L9.
- Mobasher, B., Sharples, R. M.& Ellis, R. S. 1993, MNRAS, 263, 560
- Osterbrock, D.E. 1974, Astrophysics of Gaseous Nebula (San Francisco; Freeman).
- Pascarelle, S.M., Windhorst, R.A., Driver, S.P., Ostrander, E.J. & Keel, W.C. 1996, ApJ, 456, L21.
- Rauch, M., Haehnelt, M.G., & Steinmetz, M. 1997, ApJ, submitted.

- Readhead, A.C.S., Taylor, G.B., Pearson, T.J., & Wilkinson, P.N. 1996, *ApJ*, 460, 634.
- Rottgering, H.J.A., Lacy, M., Miley, G.K., Chambers, K.C., & Saunders, R. 1994, *A&AS*, 108, 79.
- Schechter, P. 1976, *ApJ*, 203, 297
- Spinrad, H., et al. 1993 in *Observational Cosmology*, ASP conf. ser. 51, p.585
- Thompson, D., Mannucci, F. & Beckwith, S.V.W. 1996, *AJ*, 112, 1794.
- van Ojik, R., Rottgering, H.J.A., Miley, G.K., Bremer, M.N., Macchetto, F., & Chambers, K.C.
1994, *A&A*, 289, 54.
- van Ojik, R., Rottgering, H.J.A., Miley, G.K., & Hunstead, R.W. 1997, *A&A*, 317, 358.
- van Ojik, R., Rottgering, H.J.A., Carilli, C.L., Miley, G.K., Bremer, M.N., & Macchetto, F. 1997,
A&A, in press.
- Veilleux, S. & Osterbrock, D.E. 1987, *ApJS*, 63,295.
- Young, J.S. & Scoville, N.Z. 1991, *ARA&A*, 29, 581.

Figure Captions

Fig. 1.— A mosaic of the K-band images of field around 4C +19.71. North is up and east is to the left. The radio galaxy and all the detected objects in the field are marked as they are identified in Table 1. Components “a” (at 0.0,0.0) and “b” of the radio source, as first identified by Eales & Rawlings (1996), are also marked.

Fig. 2.— Small ($20'' \times 20''$) sub-frames of the K-band mosaic (left) and narrow band mosaic (right) of the 4C +19.71 field. In both cases, north is up and east is to the left. The positions of components “a” and “b” are indicated in the K-band image. A vertical bar has been drawn within the narrow-band frame indicating a projected physical scale of 25 kpc at the redshift of 4C +19.71. The white crosses in the narrow-band frame mark the locations of the 1465 MHz radio lobes as mapped by Rottgering et al. (1994), assuming they are centered on component “a” of 4C +19.71.

Fig. 3.— Color magnitude diagram for the sources in the 4C +19.71 field. The broad-band K minus narrow band color (K-NB) is plotted against the broad-band K magnitude. All sources from Table 1 are included as measured through a $2.0''$ diameter circular aperture, excluding those with uncertainties in the measured narrow-band magnitude of more than 50%. The radio galaxy, measured at two locations as defined in the text, has a significant excess in the narrow band filter. For reference, the horizontal dotted and dot-dashed lines correspond to the observed K-NB colors of a $z = 3.594$ source with a rest frame emission-line equivalent width of 50\AA and 100\AA , respectively.

Objects in the 4C +19.71 Field

Name	K mag	Position E,N(″)
G2	15.39±0.02	+14.6,−12.0
G1	16.02±0.02	+18.7,−12.8
star A	16.10±0.02	+3.3,−11.0
G3	16.53±0.02	+13.0,−16.4
star B	16.66±0.02	+18.4,+8.9
G4	16.97±0.02	−20.0,−8.1
star C	17.36±0.02	−20.7,−14.2
4C+19.71a	20.14±0.05	0.0,0.0
4C+19.71b	21.41±0.16	+0.3,+3.6
G5	18.94±0.03	+2.1,−7.0
obj 10	19.35±0.07	+12.7,−30.8
G8	19.37±0.07	−7.5,+24.5
obj 9	19.70±0.05	−13.3,+12.3
G7	19.76±0.05	+10.5,+10.1
G6	19.78±0.05	−2.3,+4.4
obj 11	20.62±0.11	−15.9,−5.4
obj 12	20.65±0.09	+16.5,+0.3

Table 1: Near infrared magnitudes of the objects in the 4C +19.71 field. All values are measured in 2.0″ circular beams. Column 3 is the offset of each object, in arcseconds, from the position of the center of the radio galaxy (defined as component “a” in Figs. 1 and 2). Note that the K band magnitudes of 4C +19.71 given in this table are as measured through the broad band filter, uncorrected for the [OIII] emission-line flux (see text).

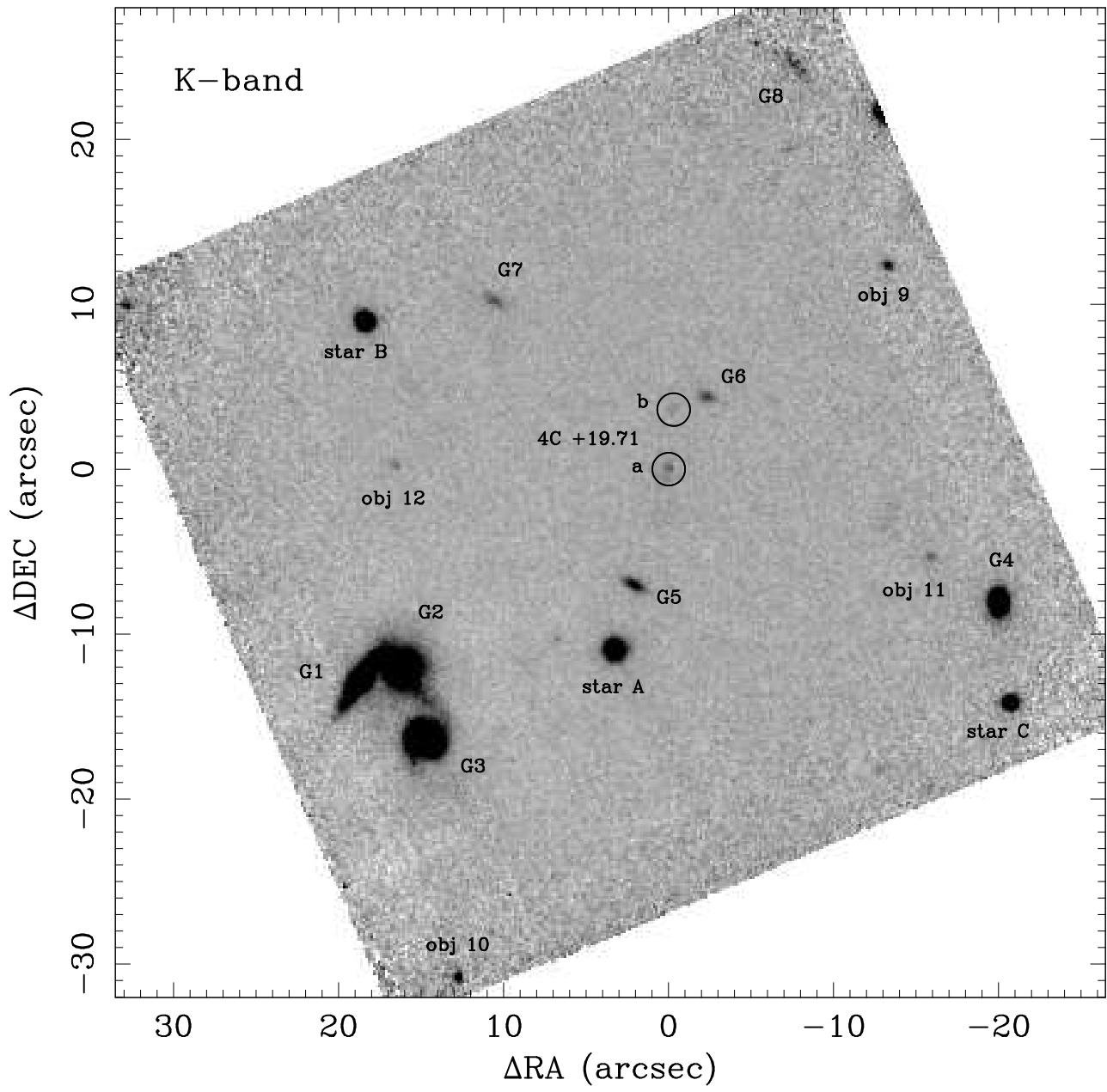


Fig. 1

4C +19.71

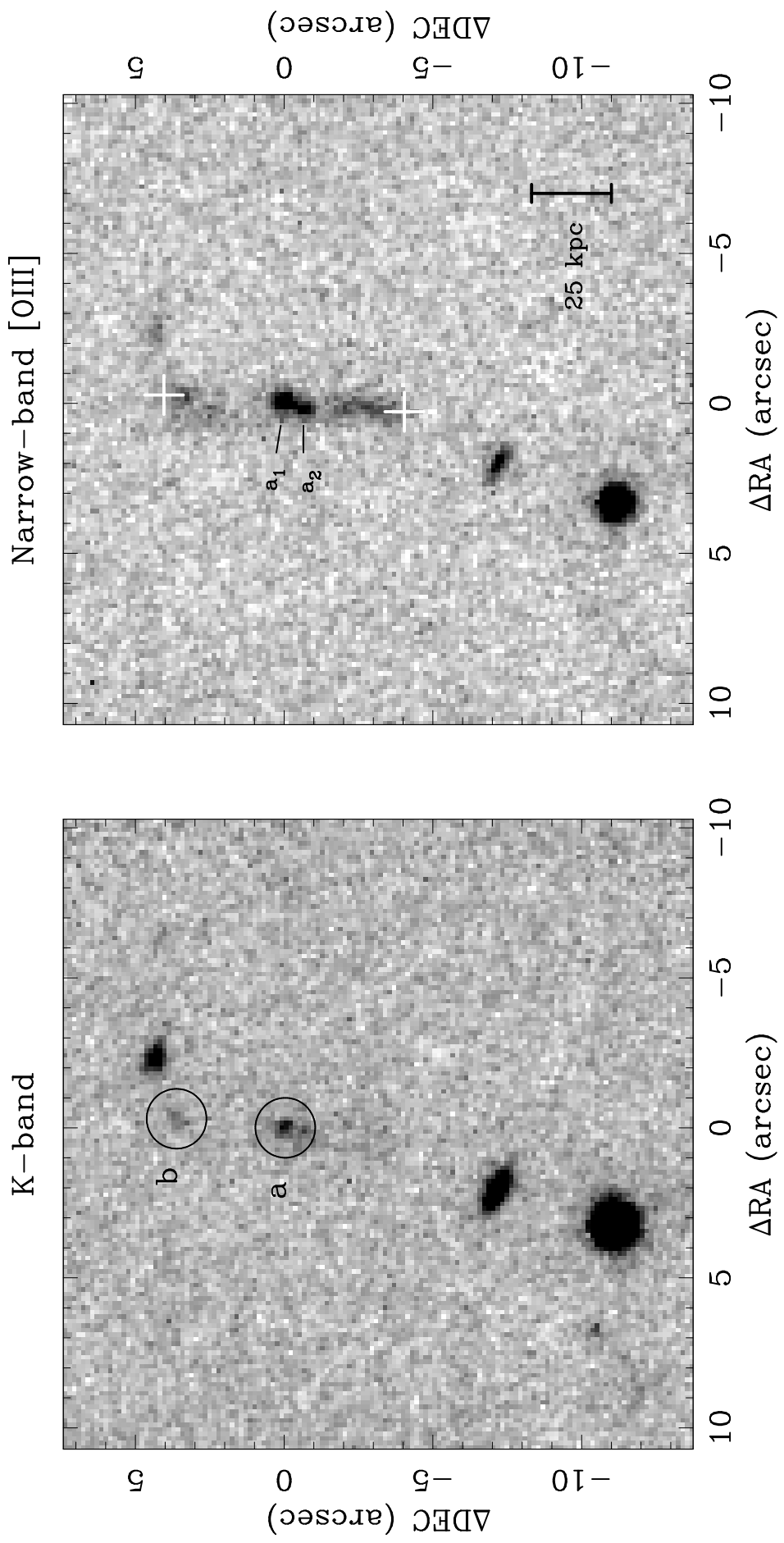


Fig. 2

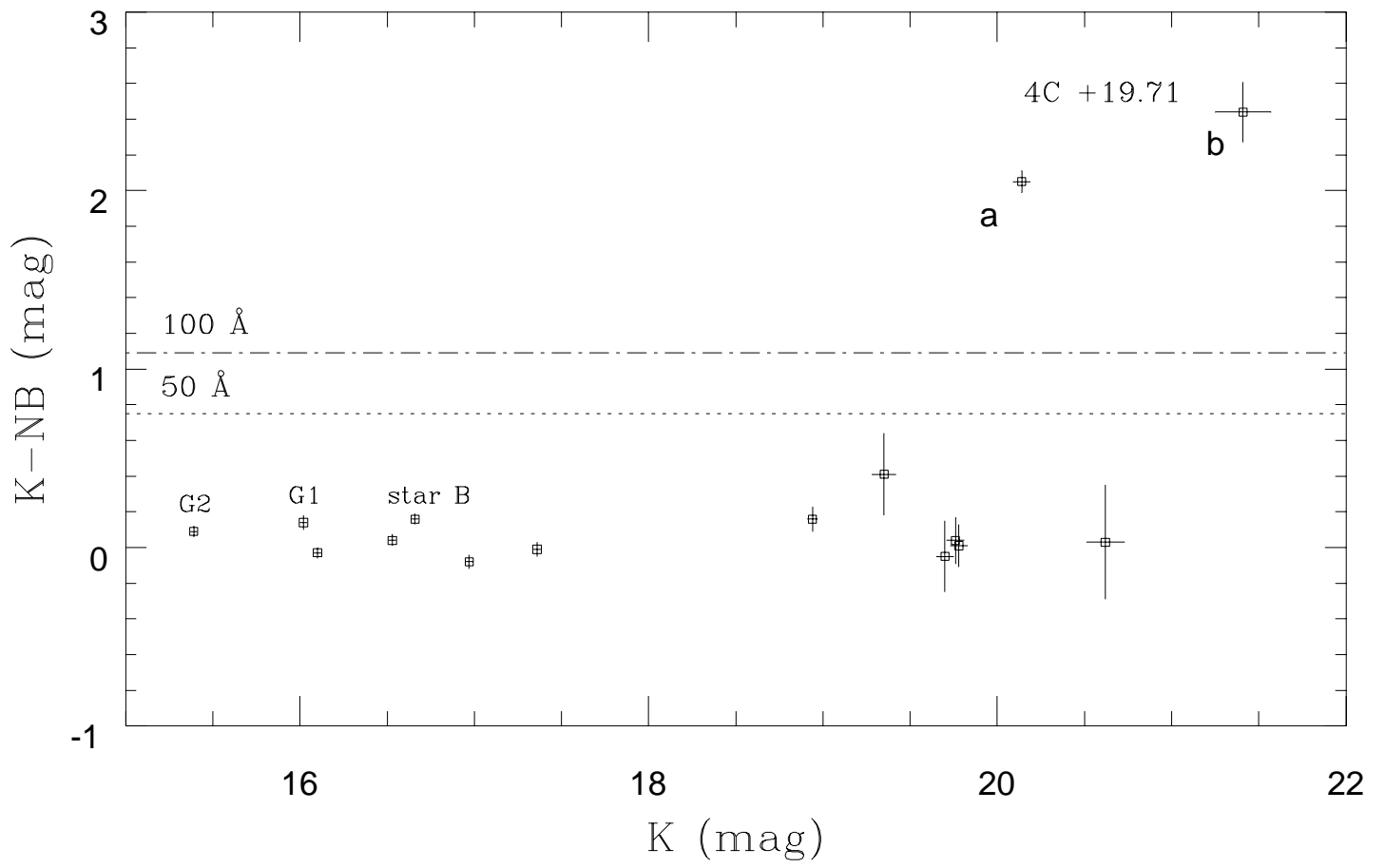


Fig. 3